Journal of Applied Polymer Science

Formation of Melt and Solution Spun Polycaprolactone Fibers by Centrifugal Spinning

Nicole E. Zander
US Army Research Laboratory, Weapons and Materials Research Directorate, Aberdeen Proving Ground, Maryland 21005
Correspondence to: N. E. Zander (E-mail: nicole.e.zander.civ@mail.mil)

ABSTRACT: Nano- and microfibers have a myriad of applications ranging from filtration, composites, energy harvesting, to tissue engineering and drug delivery. Electrospinning, the most common method to produce such fibers, has many limitations including low fiber output and solvent dependency. Centrifugal spinning is a new technique that uses centrifugal forces to form nano- and microfibers both from solution and the melt. In this work, the effect of melt temperature, collector distance, rotation speed, and concentration (for polymer solutions) of polycaprolactone were evaluated with respect to fiber morphology, diameter, alignment, and crystallinity. The fiber diameter generally decreased with increasing rotation speed and reduced concentration. Crystallinity for spun fibers decreased compared to the bulk polymer. Fiber alignment was improved with rotation speed for the melt-spun fibers. The fiber mats were evaluated as tissue scaffolds with neuronal PC12 cells. The cells adhered and extended neurites along the fibers for both melt and solution-spun scaffolds. © 2014 Wiley Periodicals, Inc. J. Appl. Polym. Sci. **2015**, *132*, 41269.

KEYWORDS: biocompatibility; crystallization; fibers; morphology; polyesters

Received 13 May 2014; accepted 14 July 2014
DOI: 10.1002/app.41269

INTRODUCTION

The high surface area to volume ratio and superior mechanical performance of nanofibers makes them attractive candidates for improving the function of numerous devices and materials.[1] Nanofibers are widely used in a variety of research fields, including sensing, energy storage/harvesting, filtration, composites, and tissue engineering. A number of processing techniques have been used to prepare nanofibers including drawing, template synthesis, phase separation, self-assembly, and electrospinning.[2–8] All of the aforementioned techniques have limitations ranging from not being able to generate continuous nanofibers (template synthesis) to requiring multiple steps (phase separation and self-assembly) to low fiber output.

Electrospinning is the most widely used method to generate continuous nanofibers and is a process in which the spinning solution is forced though a needle that is charged at high voltage. Electrostatic repulsion causes the pendant droplet to spread, and a jet is ejected when the surface tension is overcome. The jet then undergoes a series of bending instabilities that result in ultra-thin fiber diameters due to the stretching involved in this process.[9] There are many advantages to the electrospinning process such as the simplicity and versatility of the technique, and the low cost (minimal equipment needed). But the low fiber production rates (typically 0.2 g h^{-1} for lab scale), high voltage (>10 kV), solvent limitations (based on dielectric constant), and minimal melt-spinning capability limit the true scalability of this technique.[10]

A new approach to nanofiber formation known as centrifugal spinning, Forcespinning™, or rotary jet spinning overcomes many of the drawbacks of the electrospinning process.[11–13] Centrifugal spinning employs a rotary polymer source that stretches and elongates the polymer jet, rather than high voltage, enabling fiber formation with non-conductive polymers via this process.[11] Centrifugal spinning units with a heater (as displayed in Figure 1) can form fibers from the melt, eliminating toxic solvents from the process, and enabling a wider variety of polymer materials to be spun into fibers (including insoluble polymers). Production rates are significantly higher, up to 300 g h^{-1} for a Forcespinning™ benchtop unit, and thus could be more easily scaled to high rate nanofiber production. The Nanospider™, a commercialized electrospinner that uses spinning electrodes in place of needles, has much higher fiber outputs, but still considerably less than a Forcespinning™ unit.[14] The range of polymers that can be spun into fibers is just beginning to be explored. Badrossamay et al. spun fibers from PLA, PEO and gelatin solutions.[13] Senthilram and McEachin have examined spinning polycaprolactone (PCL) from solution.[10,15] PCL is a biocompatible, biodegradable, FDA-approved biomaterial with

Additional Supporting Information may be found in the online version of this article.

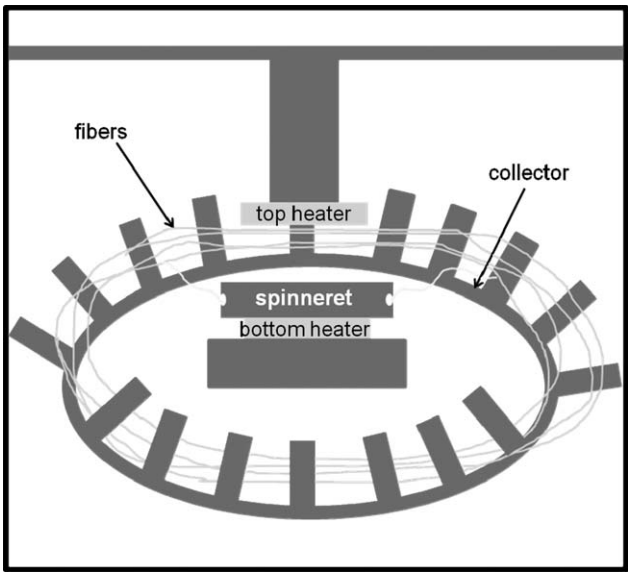

Figure 1. Schematic of Forcespinning™ system with melt spinneret. Polymer is inserted into spinneret and heated with top and bottom heaters. Top heater is raised when desired melting temperature is reached, spinneret is rotated and fibers are collected on arc collector.

good mechanical properties. Nanofibrous scaffolds of the material have been widely used in tissue engineering to support the growth and differentiation of various cells types.[16–19] Yet, the majority of tissue scaffolds are made using the electrospinning rather than centrifugal spinning process, and hence scalability of these materials is limited. A method to improve the fiber output is needed to advance the employment of these scaffolds beyond basic research use. Here, both melt and solution spinning of PCL were examined using a commercial Forcespinning™ benchtop system. The effect of parameters such as rotation speed, collector/working distance (WD), solution concentration and melting temperature on fiber morphology and crystallinity were examined. The ability of centrifugally spun fibers to act as tissue scaffolds was evaluated using neuronal PC12 cells.

MATERIALS AND METHODS

Materials

Methylene chloride, paraformaldehyde, bovine collagen type I and Triton X-100 were purchased from Sigma–Aldrich and used as received. PCL, 3-mm pellets with an average molecular weight of 40 kDa, was obtained from Polysciences, Inc. RPMI 1640, Dulbecco Modified Eagle's Medium (DMEM), horse serum, fetal bovine serum, calf serum, bovine serum albumin (BSA), phosphate buffered saline (PBS), and antibiotic/antimycotic were obtained from Fisher Scientific. Rhodamine phalloidin was obtained from Life Technologies. PC12 cells were obtained from American Type Culture Collection.

Fiber Formation

Both melt- and solution-spun fibers were generated using the Fiberlab™ L1000-D purchased from Fiberio®. Melt-spun PCL fibers were prepared by adding 100–300 mg of polymer to the 20-G melt spinneret from Fiberio®. The polymer was heated with the upper and lower heaters until the temperature reached 120–250°C, as measured by a thermocouple inserted into the spinneret. The collector consisted of 6-in. high × 1/2-in. wide bars separated by 1 in., arranged in a circular pattern as displayed in Figure 1. The bars were placed between 10 and 14 in. from the spinneret orifice. The spinneret was rotated between 8000 and 18,000 rpm for 30 s to generate fibers on the collector. Fibers were collected either on aluminum foil placed between selected bars or circular glass coverslips. The dynamic viscosity of the melt was determined using an Anton Paar Physica MCR 501 rheometer.

Solution-spun PCL fibers were prepared by dissolving the polymer at RT in methylene chloride at concentrations ranging from 10 to 20 weight percent. Approximately 1 mL of polymer solution was loaded into the solution spinneret from Fiberio® containing two 21- or 30-G 1/2 in. needles. The spinneret was rotated between 3000 and 9000 rpm for 30 s at RT to generate fibers on the arc collector, as described above. The distance between the needle tip and the collector was fixed at 12.5 cm. Fibers were collected in the same manner described above.

Protein Attachment

The fibers were vacuum dried overnight, cut to fit in 12-well plates, and thoroughly rinsed with PBS. To improve the biocompatibility of the scaffolds, physically adsorbed collagen was attached by immersing the mats in a 50 μ5;g mL^{-1} solution at 4°C overnight. Scaffolds were then washed thoroughly with PBS and sterilized overnight by immersing in a sterile solution of 2% antibiotic/antimycotic in PBS. Samples were kept sterile for cell culture.

Characterization of Scaffolds

The morphology of the fibers was examined using a field-emission scanning electron microscope (SEM, Hitachi S-4700) in the secondary-electron mode, using a mixture of upper and lower detectors. An accelerating voltage of 2 kV was maintained in order to prevent surface damage to the substrate. Before observation, the samples were vacuum dried and sputter coated with gold-palladium. Several areas were imaged in order to examine the uniformity of the fiber diameters. Fiber diameters were measured using image analysis software (Image J v 1.34, National Institutes of Health). Fiber alignment was quantified using Image J by taking a Fast Fourier Transform (FFT) of the SEM image and using the Oval Plot Profile Plug-in. The X, Y data was imported into Casa XPS software (v 2.3.15) for peak fitting. The normalized maximum intensity was determined by dividing the maximum intensity by an average baseline value and plotted against spinneret rotation speed.

Thermal properties were measured on a TA Instruments DSC with a heat/cool/heat program. All samples were heated at 5°C min^{-1} to 120°C, cooled 10°C min^{-1} to −80°C, and then heated again at 5°C min^{-1} to 120°C. DSC data was processed using Universal Analysis software. The percent crystallinity of the samples was determined from the experimental heat of fusion using 139.5 J g^{-1} as the heat of fusion from a 100% crystalline PCL sample.

Surface compositional analysis was performed using a Kratos Axis Ultra 165 X-ray photoelectron spectroscopy (XPS) system

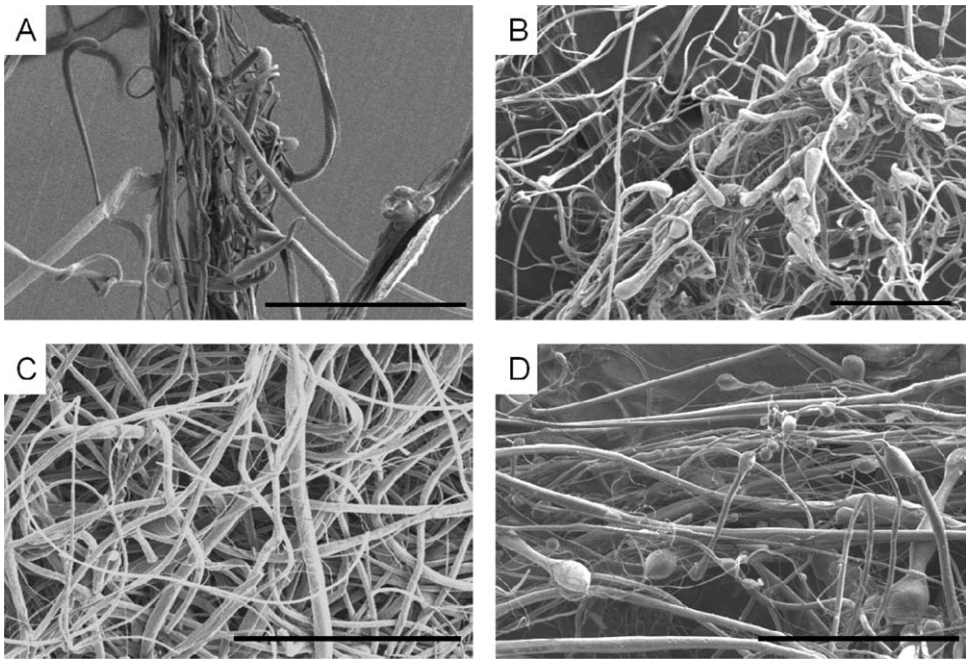

Figure 2. Scanning electron micrographs of melt-spun polycaprolactone fibers spun at different temperatures. (A) 120°C, (B) 140°C, (C) 200°C, (D) 250°C. Scale bar denotes 300 μm. Rotation speed and collector distance were fixed at 14,000 rpm and 14 cm, respectively.

equipped with a hemispherical analyzer. Sampling areas of 1 mm × 0.5 mm were irradiated with a 140 W monochromatic Al Kα (1486.7 eV) beam and take-off angle of 90°. The XPS chamber pressure was maintained between 10^{-9} and 10^{-10} Torr. Elemental high resolution scans were conducted with a 20 eV pass energy for the C 1*s*, O 1*s*, and N 1*s* core levels. A value of 284.6 eV for the hydrocarbon C 1*s* core level was used as the calibration energy for the binding energy scale. Data was processed using Casa XPS software. All reported atomic percentages are the average of $n = 2$ measurements on a minimum of three replicate samples.

Culture of PC12 Cells

PC12 cells were cultured in RPMI 1640 medium supplemented with 10% heat-inactivated horse serum and 5% fetal bovine serum and 1% antibiotic/antimycotic at 37°C and 5% CO_2. Sterile fiber mats in 24-well plates were incubated in serum-free medium 2 h prior to seeding cells. For cellular assay, cells were seeded at a density of 5000 cells/well in high-glucose DMEM with 1% horse serum, 0.5% calf serum, and 1% antibiotic/antimycotic. After 24 h, 100 ng mL^{-1} NGF was added to the assay medium. Cells were fixed after 5 days and stained for confocal laser scanning microscopy (CLSM). To prepare samples for CLSM, the scaffolds were rinsed thoroughly with PBS and fixed in 4% paraformaldehyde in PBS for 20 min. Scaffolds were rinsed with PBS and cells were permeabilized with 0.2% Triton X-100 for 10 min. Nonspecific labeling was prevented by incubating samples in a blocking buffer composed of 1% BSA in PBS for 20 min. Samples were then immersed in rhodamine phalloidin (1:200) in blocking buffer for 1 h. Samples were rinsed thoroughly with PBS and kept in the dark at 4°C until analysis. Samples were imaged on a Zeiss LSM5 Pascal equipped with Epiplan-Neofluar lenses. The cells in the scaffolds were imaged with a 543 nm laser using the 10× and 20× objectives.

Cell Viability Assay

The viability and proliferation of PC12 cells on the fiber scaffolds were determined using a MTS assay after day 1, 3, and 5 of culture in a complete medium. After the specified time point, the medium was removed and the cell-seeded scaffolds were transferred to a clean 24-well plate. Clear serum-free DMEM and MTS solution were added to each well. The samples were incubated at 37°C for 3 h. Samples were analyzed with a spectrophotometric plate reader (Perkin Elmer Fusion).

Statistics

All data are expressed as mean ± standard deviation (SD) unless noted. Unpaired Student's *t* tests were conducted with a significance level of $P < 0.05$ using Origin v 8.5.

RESULTS

Fiber Morphology: Melt-Spun Fibers

Nanometer to micrometer-sized PCL fibers were formed using the centrifugal spinning process. The effect of the temperature on fiber formation and quality was evaluated at temperatures ranging from 100 to 250°C. Although the melting temperature for the PCL used in the experiments was about 60°C, very little fiber formation was observed at temperatures below 200°C due to the high viscosity. A small amount of fibers were formed at temperatures as low as 120°C, but only at very high rotation speeds. The fibers were twisted and had a large distribution in fiber diameter, as shown in Figure 2 and denoted in Table I. A significantly larger quantity of fibers was observed when the melt was heated to 200°C, the optimal melt-flow viscosity determined in this work [Figure 2(C)]. The fibers were also less beady and more uniform in diameter and morphology. The

Table I. Fiber Diameter of Melt-Spun Polycaprolactone Fibers Based on Spinning Temperature

Temperature (°C)	Viscosity (Pa s^{-1})	Fiber diameter (μm)
120	158.1	9.67 ± 4.9
140	130.4	8.80 ± 3.1
200	43.3	7.05± 1.1
250	17.8	12.82 ± 8.4

All fibers were prepared by spinning at 14,000 rpm for 30 s with collector distance fixed at 14 cm.

fiber diameter decreased as well, most likely due to the lower viscosity of the melt at the higher temperature. Increasing the spinning temperature further did not improve fiber quality or decrease the average diameter. Instead, fibers contained more beads, were thicker in diameter, and had a much larger fiber diameter size distribution due to the bimodal distribution of small and large fibers [Figure 2(D)]. In addition, the mechanical integrity of the mat was noticeably decreased, likely due to polymer degredation.

The effect of the distance between the spinneret orifice opening and the collector was also examined. Fibers were spun at 200°C and working distances of 10, 12, and 14 cm, and there was no statistical difference in fiber diameters (see Table II). However, there was a difference in the morphology of the fibers collected (Figure 3). The size distribution was larger for the fibers collected at a shorter working distance, and the fibers were also more twisted, broken, and beady.

The rotation speed of the melt spinneret was also varied between 6000 and 18,000 rpm to determine the optimal rotation speed for uniform fiber morphology and alignment. Speeds slower than 8000 rpm were insufficient to eject the molten polymer from the spinneret. A few discontinuous (broken) fibers were observed at the 8000 rpm rotation speed [Figure 4(A)]. A high density of fibers were observed for both the 14,000 and 18,000 rpm rotation speeds [Figure 4(C,D)]. As discussed above, fiber quality and uniformity were good for the fibers spun at 14,000 rpm and 200°C. On the other hand, the fibers formed at 18,000 rpm contained many beads, most likely due to the extremely rapid solidification time between ejection from the spinneret to deposition on the collector and possibly stick-slip flow through the orifice. The fiber diameters decreased with rotation speed and ranged from 6.1 ± 3.9 to 10.2 ± 3.3 μm (18,000–8000 rpm), as shown in Figure 5. The fiber diameter distributions were quite large for all except the fibers formed at 14,000 rpm, which appears to be the best speed to minimize bead formation and optimize fiber uniformity.

Fiber Morphology: Solution-Spun Fibers

Fibers were also prepared by centrifugal spinning from solution. PCL concentrations ranging from 10 to 20 wt % in methylene chloride were evaluated at rotation speeds of 3000, 6000, and 9000 rpm using 21-G and 30-G needles. No fibers were formed at 3000 rpm with the 21-G needles, but fibers were formed at 6000 and 9000 rpm for the 15 wt % solution. Using 30-G needles, no fibers were formed at 3000 rpm for the 10 and 20 wt % solutions, but a small amount of fibers were generated for the 15 wt % solution. Fibers were formed for all concentrations at 6000 and 9000 rpm with the latter needle size. Images of fiber formed using 30-G needles are displayed in Figure 6. Fiber diameter ranged from 0.81 ± 0.5 to 3.45 ± 1.7 μm, as can be seen in Figure 5 and in general decreased with concentration and faster rotation speed.

Fiber Alignment

The fiber alignment was calculated from pixel intensity patterns from Fast Fourier Transforms (FFT) of fiber SEM images. A high concentration of pixels perpendicular to the dominate fiber axis was indicative of fiber alignment. For the melt-spun fibers, the fiber alignment did not show a clear trend with rotation speed due to the data point at 10,000 rpm, as can be seen in Figure 7, but generally increased with rotation speed. By eye, the fibers spun at 18,000 rpm appeared to have very high alignment [Figure 4(D)], but the FFT pattern showed only modest alignment, probably due to the high concentration of circular beads and waviness of the fibers. Data for the alignment of solution spun fibers is displayed only for fibers generated at 6000 and 9000 rpm because fibers were not formed for all concentrations at other rotation speeds. Thus, it is difficult to make conclusions about the effect of rotation speed on solution spun fibers.

Thermal Analysis

DSC was utilized to study the crystallinity of spun fibers. Heat flow-temperature curves are displayed in Figure 8 and tabulated results in Table III. It is evident that the melting temperature decreased for the spun fibers compared to the bulk. There was little variation between fibers prepared with different conditions, with melting temperatures ranging from 57.1 to 58.9°C. The peak crystallization temperature was higher for the spun fibers compared to the bulk, and appeared to increase slightly with rotation speed. The highest peak crystallization temperatures were observed for the melt spun fibers with 10 and 12 cm working distances. The crystallinity was calculated using the following equation:

$$X_c = \frac{\Delta H_m - \Delta H_c}{\Delta H_f}$$

where ΔH_m is the enthalpy of fusion, ΔH_c is the enthalpy of cold crystallization, and ΔH_f is the enthalpy of fusion of a 100% crystalline sample (139.5 J g^{-1}). The DSC data shows a decrease in crystallinity for the fibers compared to bulk PCL. The crystallinity also decreased with rotation speed except for the melt-spun fibers, which showed an initial decrease for fibers formed at 14,000 rpm compared to 10,000 rpm followed by an

Table II. Fiber Diameter of Melt-Spun Polycaprolactone Fibers Based on Collector Distance

Collector distance (cm)	Fiber diameter (μm)
10	8.20 ± 5.8
12	8.33 ± 4.4
14	7.05± 1.1

All fibers were prepared by spinning at 14,000 rpm at 200°C for 30 s

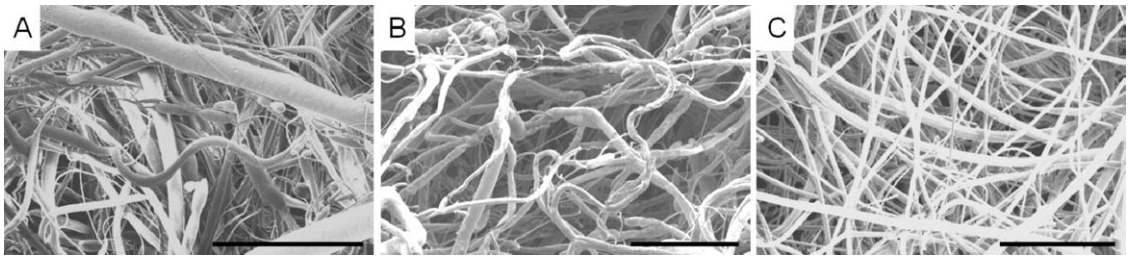

Figure 3. Scanning electron micrographs of melt-spun polycaprolactone fibers spun with different collector distances. (A) 10 cm, (B) 12 cm, (C) 14 cm. Scale bar denotes 200 μm. Rotation speed and temperature were fixed at 14,000 rpm and 200°C, respectively.

increase for the fibers formed at 18,000 rpm. Working distance also had an effect on crystallinity. Fibers formed at shorter working distances had higher crystallinity. Solution concentration did not appear to have a strong influence on crystallization.

Cell Growth

After optimization of processing parameters to generate uniform fiber mats using centrifugal spinning, the mats were evaluated for their potential to support cellular growth. PC12 cells, derived from the pheochromocytoma of the rat adrenal medulla, undergo neuron-like differentiation. Thus, they are a useful model system to study the ability of the fiber mat to act as a scaffold for tissue growth. Melt- and solution-spun fibers were collected on glass coverslips and coated with collagen. The attachment of collagen was verified with X-ray photoelectron spectroscopy (see Supporting Information). The PCL C 1s spectrum contains three components consisting of the hydrocarbon, ether of the ester and the carboxylic. Attachment of the protein introduced a fourth component for the amide bond. The atomic percent nitrogen for the solution-spun fibers (15% PCL, 6000 rpm, 12.5 cm WD) was determined to be 7.4% $\pm$ 0.6% for the fibers with attached collagen after rinsing with PBS. Before performing differentiation studies, the viability of PC12 cells on the pure and collagen PCL fibers were evaluated with a standard MTS assay which correlated absorbance with the number of viable cells (see Supporting Information). The viability was higher only by day 5 for the collagen PCL fibers, but the number of viable cells increased from day 1 to 5. Figure 9 displays images of the neurons grown on the mats for 5 days. Figure 9(A,B)

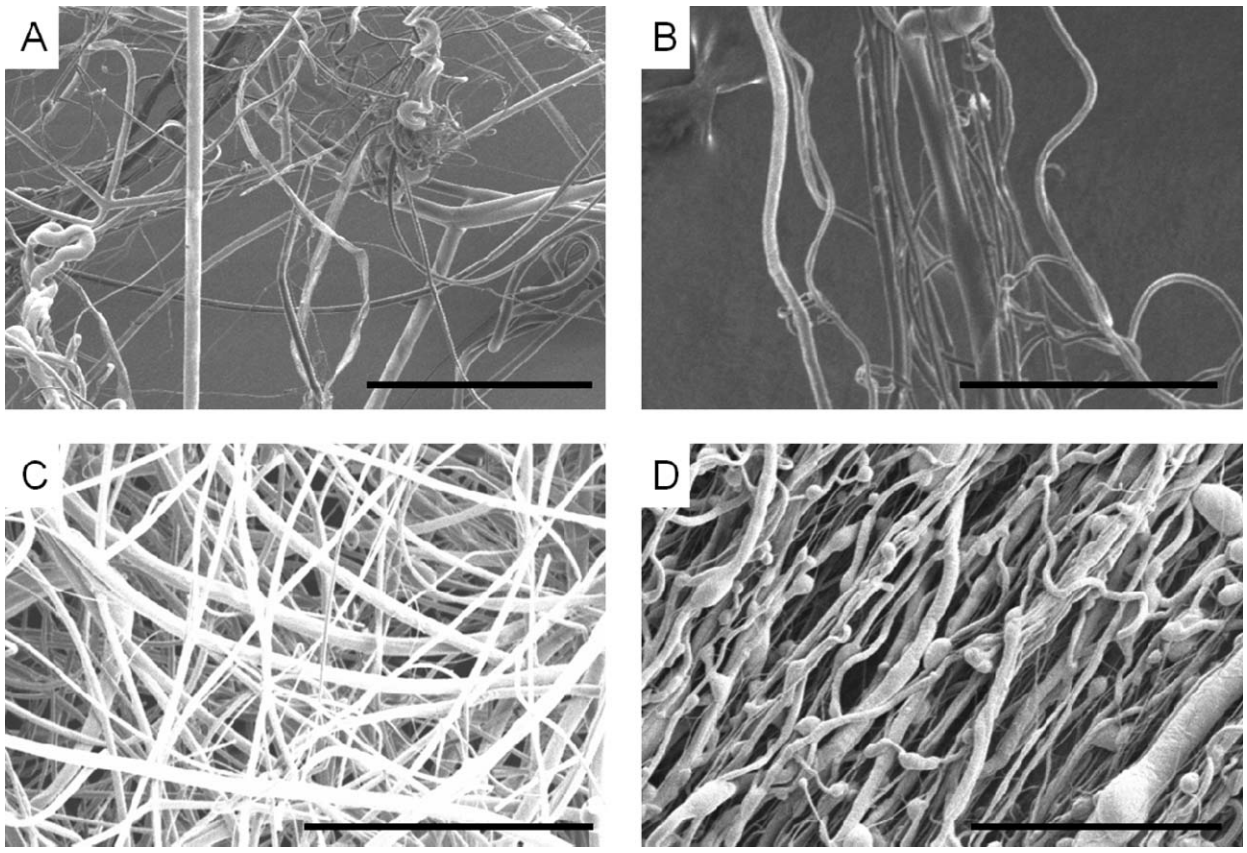

Figure 4. Scanning electron micrographs of melt-spun polycaprolactone fibers spun at various rotation speeds. (A) 8000 rpm, (B) 10,000 rpm, (C) 14,000, (D) 18,000. Scale bar denotes 300 μm. Temperature and collector distance were fixed at 200°C and 14 cm, respectively.

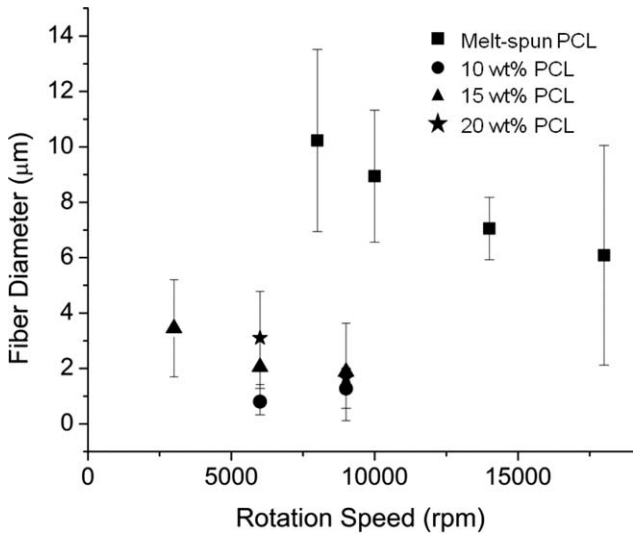

Figure 5. Fiber diameter of polycaprolactone fibers prepared by centrifugal spinning. Squares denote fibers prepared from the melt, circles denote fibers prepared from 10 wt % PCL solution, triangles denote fibers prepared from 15 wt % PCL solution, stars denote fibers prepared from 20 wt % PCL solution. Melt-spun fibers were spun at 200°C with a WD of 14 cm. Solution-spun fibers were spun at RT with a WD of 12.5 cm.

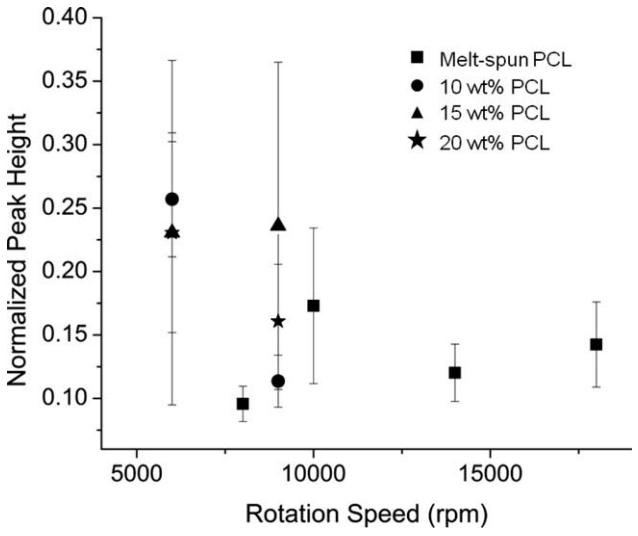

Figure 7. Fiber alignment quantification of polycaprolactone fibers prepared by centrifugal spinning. Squares denote fibers prepared from the melt, circles denote fibers prepared from 10 wt % PCL solution, triangles denote fibers prepared from 15 wt % PCL solution, stars denote fibers prepared from 20 wt % PCL solution. Melt-spun fibers were spun at 200°C with a WD of 14 cm. Solution-spun fibers were spun at RT with a WD of 12.5 cm.

show a high level of differentiation and spreading on the solution- and melt-spun mats, respectively. Figure 9(C) displays a composite image of the cells and fibers to show that they are attached inside the fiber mat.

DISCUSSION

PCL fibers were preparing using centrifugal spinning both from the melt and solution. A host of parameters including melting temperature, rotation speed, collector distance, and solution concentration were evaluated to optimize fiber formation. The fiber diameter for melt-spun fibers were in the micrometer rather than nanometer range, regardless of processing parameters studied. Dalton et al. attributed large fiber diameters in melt-electrospinning to the high melt viscosity. The addition of a viscosity reducing additive substantially reduced the diameter of melt electrospun PCL fibers and improved fiber quality.[20] The melting temperature did not have a large effect on fiber diameter in general, but did affect the fiber quality. Fibers formed at <200°C were twisted, beady, had a large fiber size distribution, and of low yield. Fiber diameter was also higher than those formed at 200°C. Possibly, at the lower temperatures the viscosity was too high for uniform flow. Thus, the higher viscosity solution resulted in larger, sometimes broken fibers

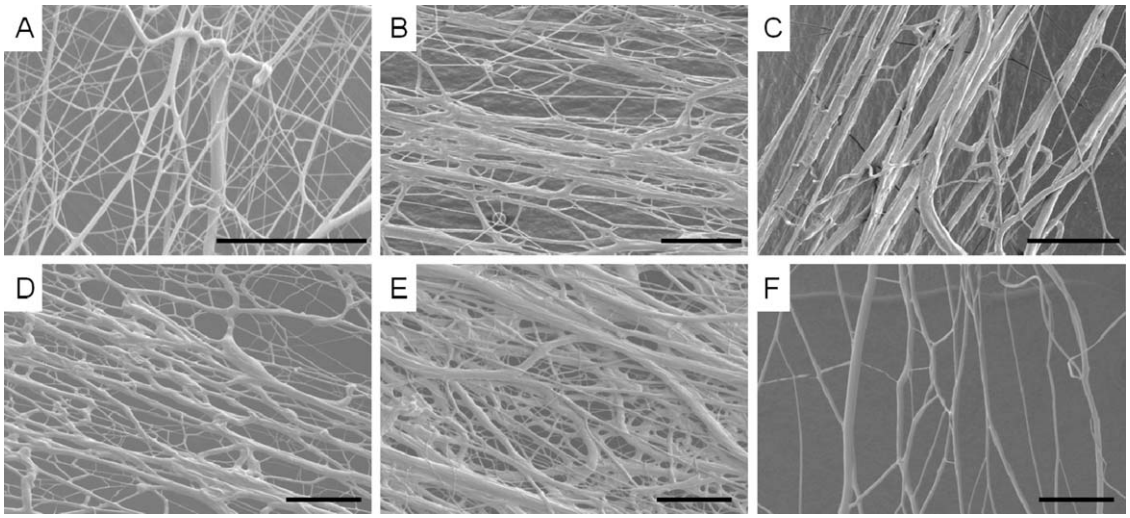

Figure 6. Scanning electron micrographs of solution-spun polycaprolactone fibers using 30-G needles. (A) 10 wt % PCL, 6000 rpm; (B) 15 wt % PCL, 6000 rpm; (C) 20 wt % PCL, 6000; (D) 10 wt % PCL, 9000; (E) 15 wt % PCL, 9000 rpm; (F) 20 wt % PCL, 9000 rpm. Scale bar denotes 50 μm. The collector distance was fixed at 12.5 cm.

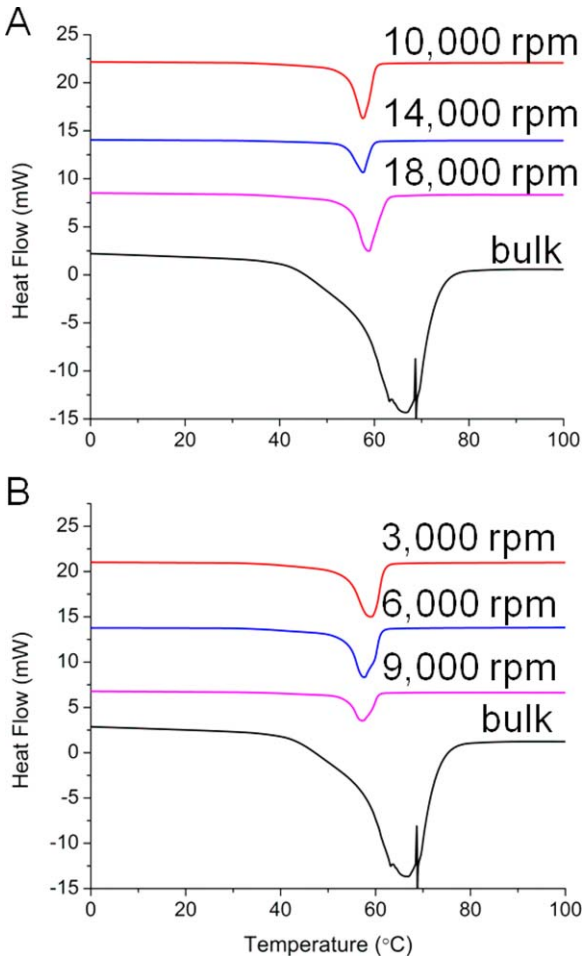

Figure 8. Melting endotherms for bulk polycaprolactone and fibers prepared by centrifugal spinning. (A) Melt-spun fibers (200°C), (B) solution spun fibers (15 wt %). Spinneret rotation speeds are denoted in the figure. [Color figure can be viewed in the online issue, which is available at wileyonlinelibrary.com.]

and necking-type behavior giving both very thick and thin fibers. Li et al. spun PCL fibers from the melt using a laser as the heat source. An increase in laser current decreased fiber diameter and improved fiber quality.[21] Melting the polymer at 250°C (above the onset degradation temperature) did not serve to further improve fiber quality, but resulted in substantial beading possibly due to chain scission, resulting in too low viscosity for uniform flow. In addition, many broken fibers were observed, likely for the same reason. The effect of collector distance was not found to control fiber diameter, in agreement with Li et al. and Lu et al., but did affect fiber quality.[21,22] Larger fiber size distributions and an increase in beady and twisted fibers were observed for the shorter working distances. Shorter distances mean that they fibers have less time to solidify and undergo relaxation, thus accounting for the beads and helical morphology.

Rotation speed of the spinneret in general served to reduce fiber diameter and improve quality. At the lower rotation speeds, viscosity is an impediment to flow and only a portion of the melt was ejected from the spinneret orifice. The large size distribution at the lower speeds could be attributed to the non-uniform flow. At the fastest rotation speeds, variable forces act on the fiber formation including stick-slip flow and uneven feeding/ejection of the melt. This leads to a large size distribution such as that observed for the fibers formed at the 18,000 rpm rotation speed, which contained very fine uniform fibers and larger fibers with varied size of beads. The high level of beads could also be ascribed to the rapid cooling and solidification of the melt.

Fiber uniformity/quality varied less with the fibers formed from solution. Faster rotation speeds typically decreased fiber diameter, in agreement with McEachin et al. and Lu et al., but did not improve fiber alignment.[10,22] Fiber formation was initially attempted with a 21-G needle, but fibers were only generated from the 15 wt % solution. The orifice was likely too large to allow adequate drawing for fiber formation, resulting in droplet spraying rather than fiber spinning.[23] Melt-spun fibers, on the other hand, were only produced with the 20-G spinneret and not the 30-G spinneret. Because of the much higher viscosity of the melt, more force is required to eject the polymer from the spinneret. Smaller length/diameter (L/D) aspect ratios improve polymer ejection by increasing the exit velocity. The higher viscosity of the melt also explained the larger fiber diameters observed compared to the solution spun fibers. In addition, fibers were not formed at rotation speeds $<$5000 rpm (except for the 15 wt % solution). Padron et al. modeled fiber trajectories and found that as the viscosity of the material increased, the angular velocity required to collect fibers also increased.[23] For a 10 wt % polyethylene oxide solution, at rotation speeds below 4500 rpm, ejected polymer was pulled inward and collected on the rotating shaft rather than forming fibers on the collector. Based on the aforementioned work, fibers were expected to form more readily at lower rotation speeds for lower viscosity solutions, which was observed in the case of the 15 wt % solution.

The alignment of fibers was expected to improve with faster rotation speeds, a phenomenon observed in electrospinning (collector speed rather than spinneret speed). In general, alignment was not very high, but the melt spun fibers appeared to follow this trend except for the fibers formed at 10,000 rpm. These fibers had a large error bar for normalized peak height of FFT pixel intensities due to the cross-like orientation of the fibers. Mary et al. generated highly aligned fibers from solution using an air-stream controller on their spinneret at fairly low rotation speeds (2000 rpm).[24] Thus, methods to control airflow, in addition to adjusting rotation speed, might aid in improving fiber orientation.

In terms of thermal changes, the crystallinity and melting point decreased for the spun fibers compared to the bulk. The trend appears counterintuitive in that the extensional flow/fiber drawing should serve to increase crystallinity, particularly at faster rotation speeds, but in fact does the opposite. McEachin et al. and Raghavan et al. observed the formation of an oriented mesophase for centrifugal solution-spun PCL fibers and melt-spun polypropylene (PP) fibers, which resulted in incomplete crystallization.[10,25] But, Lu et al. reported an increase in the crystallinity of polyacrylonitrile (PAN) fibers centrifugally spun from

Table III. Thermal Analysis of Bulk Polycaprolactone and Fibers Prepared by Centrifugal Spinning

	Crystallization		Melting		
Sample	T_c (°C)	ΔH_c (J g^{-1})	T_m (°C)	ΔH_m (J g^{-1})	% Crystallinity
Bulk PCL	22.7	61.1	68.8	87.9	19.1
Melt-10,000 rpm	29.3	66.3	57.6	80.4	10.1
Melt-14,000 rpm	30.4	69.6	57.5	76.6	5.0
Melt-18,000 rpm	29.8	64.6	58.7	80.5	11.1
Melt-10 cm WD	32.7	59.3	58.6	70.4	8.0
Melt-12 cm WD	34.6	62.7	58.0	72.8	7.2
Melt-14 cm WD	30.4	69.6	57.5	76.6	5.0
10%-6000 rpm	28.2	62.8	57.7	76.8	10.0
10%-9000 rpm	31.0	62.4	58.6	71.8	6.7
15%-3000 rpm	30.0	61.8	58.9	76.3	10.4
15%-6000 rpm	30.3	63.5	57.5	76.8	9.5
15%-9000 rpm	30.0	58.2	57.1	70.5	8.8
20%-6000 rpm	30.6	65.5	57.8	82.0	11.8
20%-9000 rpm	30.8	61.5	57.3	74.4	9.3

Melt = melt-spun at 200°C, percentages denote wt % PCL for solution spun fibers, WD = working distance, T_c = peak crystallization temperature, ΔH_c = enthalpy of crystallization, T_m = melting temperature, ΔH_m = enthalpy of fusion. The working distance was fixed at 14 cm and 12.5 cm for melt-spun and solution-spun fibers respectively, unless noted in the table.

solution.[22] This lack of consensus and counterintuitive nature of our observed results warrents further study. Perhaps the fiber drawing is in competition with rapid cooling/solvent evaporation. Fibers formed at faster spinneret rotation speeds in general had smaller diameters and thus increased rates of cooling/solvent evaporation. X-ray scattering studies could be useful to reveal information about the size of the crystallites and whether rapid cooling leads to a decreased crystal size. Our results indicate, at least for PCL, crystallinity is primarily governed by the rate of cooling, and thus an inverse relationship between crystallinity and rotation speed. The exception to this rule was the melt-spun fibers formed at 18,000 rpm, which showed an increase in crystallinity. This disparity could be due to the extremely large fiber diameter distribution (6.1 ± 3.9 μm) and large beads (lower surface area) in the fibers, which may have decreased cooling rates. Increasing the working distance (and thus time to reach the collector) for the melt-spun fibers did not increase crystallinity. Fibers collected at shorter working distances actually had higher levels of crystallinity. Possibly, the cooling took place after the fibers reached the collector for the shorter working distances, and thus was slower allowing more crystallization to occur.

PC12 neurons successfully attached and differentiated on both the melt and solution spun fibers, with fiber diameters of 7.05 ± 1.1 μm and 2.05 ± 1.1 μm, respectively. There have been many studies on the effect of fiber diameter on cellular growth. Hsu et al. observed that fiber size (sub-micron) had a more dominant role in controlling the migration and morphology of osteoblast-like MG63 cells compared to cell growth.[26] However, Shih et al. saw very little difference between cell migration and morphology for mesenchymal stem cells based on fiber diameter (sub-micron).[27] Chen et al. found that fibroblast growth kinetics did not vary significantly for fibers in the micrometer size range.[28] The cell growth differences appear to be most prominent for nanometer sized fibers and not micrometer size fibers, such as those examined in our cellular studies. Thus, we did not select fiber diameter as a variable in these studies.

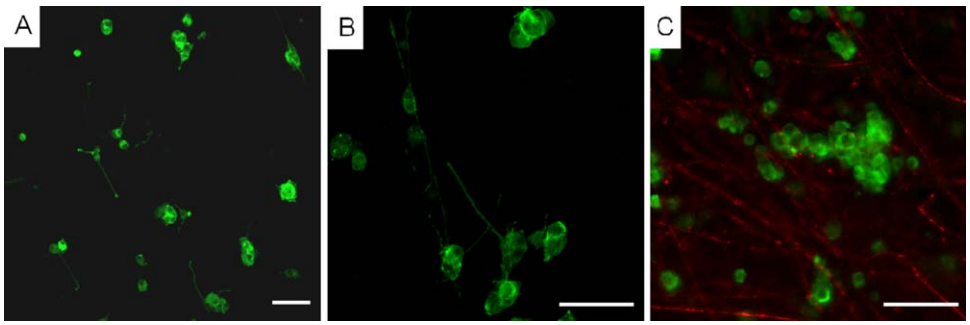

Figure 9. Confocal laser scanning microscopy images of PC12 neurons grown on polycaprolactone fibers prepared by centrifugal spinning. (A) Solution-spun (15 wt % PCL, 6000 rpm, 12.5 cm WD); (B) melt-spun fibers (200°C, 14,000 rpm, 14 cm WD); (C) melt-spun fibers two-channel image (200°C, 14,000 rpm, 14 cm WD). Scale bar denotes 100 μm. [Color figure can be viewed in the online issue, which is available at wileyonlinelibrary.com.]

CONCLUSIONS

Polycaprolactone fibers were prepared both from the melt and solution using centrifugal spinning. Processing parameters were optimized to generate uniform fibers. A heating temperature of 200°C and rotation speed of 14,000 rpm generated the best melt-spun fibers with diameter 7.0 ± 1.1 μm. Fiber diameters were smaller for the solution spun fibers, ranging from 0.81 ± 0.5 μm to 3.45 ± 1.7 μm, and generally were equivalent in quality. The fiber crystallinity was reduced compared to bulk PCL, and found to be inversely proportional to rotation speed and working distance. The melt- and solution-spun PCL fiber mats were evaluated as tissue scaffolds for PC12 neurons, and both effectively supported cell growth and differentiation. Thus, centrifugal spinning is an acceptable way to prepare tissue scaffolds. With its higher output and solvent-free capabilities, centrifugal spinning could potentially replace electrospinning as the primary method to make such materials, provided fiber diameter can be further reduced with appropriate processing parameters.

REFERENCES

1. Huang, Z.; Zhang, Y. Z.; Kotaki, M.; Ramakrishna, S. *Compos. Sci. Technol.* **2003**, *63*, 2223.
2. Ondarcuhu, T.; Joachim, C. *Europhys. Lett.* **1998**, *42*, 215.
3. Tabar, H. R. *Phys. Rep.* **2000**, *325*, 239.
4. Martin, C. R. *Chem. Mater.* **1996**, *8*, 1739.
5. Ma, P. X.; Zhang, R. *J. Biomed. Mater. Res.* **1999**, *46*, 60.
6. Liu, G. J.; Ding, J. F.; Qiao, L. J.; Guo, A.; Dymov, B. P.; Gleeson, J. T.; Hasimoto, T.; Saijo, K. *Chem. A Eur. J.* **1999**, *5*, 2740.
7. Whitesides, G. M.; Grzybowski, B. *Science* **2002**, *295*, 2418.
8. Deitzel, J. M.; Kleinmeyer, J.; Hirvonen, J. K.; Beck, T. N. C. *Polymer* **2001**, *42*, 8163.
9. Kumbar, S. G.; James, R.; Nukavarapu, S. P.; Laurencin, C. T. *Biomed. Mater.* **2008**, *3*, 34002, 1.
10. McEachin, Z.; Lozano, K. *J. Appl. Polym. Sci.* **2012**, *126*, 473.
11. Weltz, R. T.; Harnau, L.; Rauschenbach, S.; Burghard, M.; Kern, K. *Nano Lett.* **2008**, *8*, 1187.
12. Sarkar, K.; Gomez, C.; Zambrano, S.; Ramirez, M.; de Hoyos, E.; Vazquez, H.; Lozano, K. *Mater. Today* **2010**, *13*, 12.
13. Badrossamay, M. R.; Mcllwee, H. A.; Goss, J. A.; Parker, K. K. *Nano. Lett.* **2010**, *10*, 2257.
14. Elmarco. Nanospider specifications. Available at: http://www.elmarco.com/nanofiber-equipment/electrospinning-equipment-ns-lab/ (accessed April 9, 2014).
15. Senthilram, T.; Mary, L. A.; Venugopal, J. R.; Nagarajan, L.; Ramakrishna, S.; Dev, V. R. G. *Mater. Today* **2011**, *14*, 226.
16. Yoshimoto, H.; Shin, Y. M.; Terai, H.; Vacanti, J. P. *Biomaterials* **2003**, *24*, 2077.
17. Zhang, Y. Z.; Ouyang, H. W.; Lim, C. T.; Ramakrishna, S.; Huang, Z. M. *J. Biomed. Mater. Res. B* **2005**, *72B*, 156.
18. Li, W. J.; Danielson, K. G.; Alexander, P. G.; Tuan, R. S. *J. Biomed. Mater. Res. A* **2003**, *67A*, 1105.
19. Zander, N.; Orlicki, J.; Rawlett, A.; Beebe, T. *Biointerphases* **2010**, *5*, 149.
20. Dalton, P. D.; Grafahrend, D.; Klinkhammer, K.; Klee, D.; Möller, M. *Polymer* **2007**, *48*, 6823.
21. Li, X.; Liu, H.; Wang, J.; Li, C. *Polymer* **2012**, *53*, 248.
22. Lu, Y.; Li, Y.; Zhang, S.; Xu, G.; Fu, K.; Lee, H.; Zhang, X. *Eur. Polym. J.* **2013**, *49*, 3834.
23. Padron, S.; Fuentes, A.; Caruntu, D.; Lozano, K. *J. Appl. Phys.* **2013**, *113*, 024318:1.
24. Mary, L. A.; Senthilram, T.; Suganya, S.; Nagarajan, L.; Venugopal, J. *Express Polym. Lett.* **2013**, *7*, 238.
25. Raghavan, B.; Soto, H.; Lozano, K. *J. Eng. Fiber. Fabr.* **2013**, *8*, 52.
26. Hsu, Y. M.; Chen, C. N.; Chiu, J. J.; Chang, S. H.; Wang, Y. J. *J. Biomed. Mater. Res. B* **2009**, *91*, 2391.
27. Shih, Y. V.; Chen, C.; Tsai, S.; Wang, Y. J.; Lee, O. K. *Stem Cells* **2006**, *24*, 2391.
28. Chen, M.; Patra, P. K.; Warner, S. B.; Bhowmick, S. *Tissue Eng.* **2007**, *13*, 579.